Published in final edited form as:
IEEE Trans Nucl Sci. 2009 ; 56(5): 2636–2643. doi:10.1109/TNS.2009.2023444.

Quantification of the Multiplexing Effects in Multi-Pinhole Small Animal SPECT: A Simulation Study

Greta S. P. Mok,
Department of Diagnostic Radiology and Organ Imaging, The Chinese University of Hong Kong, Hong Kong

Yuchuan Wang, and
Dana-Farber Cancer Institute, Harvard Medical School, MA 02115 USA

Benjamin M. W. Tsui[Fellow, IEEE]
Department of Radiology, Johns Hopkins University, MD 21287 USA

Greta S. P. Mok: gretamok@cuhk.edu.hk; Yuchuan Wang: yuchuan_wang@dfci.harvard.edu; Benjamin M. W. Tsui: btsui1@jhmi.edu

Abstract

Our goal is to study the trade-off between image degradation and improved detection efficiency and resolution from allowing multiplexing in multi-pinhole (MPH) SPECT, and to determine the optimal pinhole number for MPH design. We used an analytical 3D MPH projector and two digitized phantoms: the mouse whole body (MOBY) phantom and a hot sphere phantom to generate noise-free and noisy projections, simulating pinhole collimators fitted with pre-studied pinhole patterns. We performed three schemes to achieve different degrees of multiplexing: 1. Fixed magnification and detection efficiency; 2. Fixed detection efficiency and changed magnification; 3. Fixed magnification and changed detection efficiency. We generated various noisy data sets by simulating Poisson noise using differently scaled noise-free projections and obtained 20 noise realizations for each setting. All datasets were reconstructed using 3D MPH ML-EM reconstruction method. We analyzed the quantitative accuracy by the normalized-mean-square-error. We evaluated the image contrast for the hot sphere phantom simulation, and also the image noise by the average normalized-standard-deviation of certain pixels for different degrees of multiplexing. Generally, no apparent artifacts were observed in the reconstructed images, illustrating the effectiveness of reconstructions. Bias increased for increased degree of multiplexing. Contrast was not significantly affected by multiplexing in the specific simulation scheme (1). Scheme (2) showed that excessive multiplexing to improve image resolution would not improve the overall trade-off of bias and noise compared to no multiplexing. However, scheme (3) showed that when comparing to no multiplexing, the trade-off improved initially with increased multiplexing by allowing more number of pinholes to improve detection efficiency. The trade-off reached a maximum and decreased with further multiplexing due to image degradation from increased bias. The optimal pinhole number was 7 for a compact camera with size of 12 cm × 12 cm and 9 for a standard gamma camera with size of 40 cm × 40 cm in this scheme. We conclude that the gains in improved detection efficiency and resolution by increased multiplexing are offset by increased image degradations. All the aforementioned factors must be considered in the optimum MPH collimator design for small animal SPECT imaging.

Index Terms

Multi-pinhole collimator; multiplexing; small animal imaging; SPECT

I. INTRODUCTION

MOLECULAR imaging of small animals especially rodents requires techniques with both high resolution and high detection efficiency. Pinhole SPECT is superior in its resolution and detection efficiency trade-off for imaging small objects in comparison with conventional parallel-hole SPECT [1]. Nevertheless its detection efficiency remains 2 to 3 orders of magnitude lower than that of the micro-PET [2]. For SPECT imaging, a single pinhole (SPH) collimator has data acquisition geometry of a cone beam. This means that complete sampling of the imaged volume is obtained only in the central transaxial slice of the object along the axis-of-rotation (AOR). Projections away from this central slice have increasing amounts of missing data for complete reconstruction, leading to gradual increase of image artifacts away from the center transaxial slice image. With an appropriate pinhole aperture arrangement, however, multi-pinhole (MPH) SPECT allows improved detection efficiency and sampling along the AOR [3], [5]. It also allows more angular sampling for each projection view. These advantages can be traded to shorten acquisition time, to lower injected dose or to improve resolution with smaller pinhole apertures.

Unlike parallel-hole or single pinhole collimators used in the clinical or preclinical arenas, there is yet no consensus on the optimal design of a MPH collimator. Primary parameters include the number and placement of pinholes, and whether or not to allow projection multiplexing or overlapping of projection data. There are two current design concepts for commercial MPH SPECT collimation. The first one uses physical septa to avoid multiplexing (Beekman *et al.* 2004, [4]). The second design allows a certain amount of multiplexing in the projection data (Schramn 2003, [5]). Other investigators also proposed using coded aperture with lots of pinholes (~ 100) and lots of multiplexing for small animal SPECT [14]. However, it is still in the research phase and its effectiveness compared to MPH SPECT is still under explored. We define the term multiplexing as the overlapping region of projections on the detector from different pinholes in a MPH collimator, appearing in the projection domain. When comparing to non-multiplexing design [Fig. 1(a)], multiplexing allows more efficient coverage of the detector surface so that more pinholes can be packed to further increase the detection efficiency [Fig. 1(b)]. It also allows improved resolution sampling and better projected intrinsic resolution for the same number of pinholes since each MPH projection can share more pixel elements [Fig. 1(c)]. However, the effects of multiplexing on the reconstructed image quality are still being explored [6], and they are crucial to optimizing collimator design for quantitative MPH SPECT imaging. Several authors discussed the role of the pinhole pattern in terms of artifacts generation [3], [8], [9], [12] and in this study, we focus on investigating how the degree of multiplexing affects the image quality. We used this approach to determine the optimal number of pinholes for both compact and conventional gamma cameras.

II. Materials and Methods

A. Simulation Setup

Simulation techniques provide an effective means to evaluate reconstructed image quality for different instrumentation designs, acquisition protocols, reconstruction algorithms or compensation methods. In this study, we simulated “focusing” MPH projections, i.e., all pinholes focused to the center of the object, using two different phantoms: (1) the digital mouse whole body (MOBY) phantom (Fig. 2(a) & [7]) that realistically models the anatomy of a normal C57BL/6 mouse with a typical activity distribution of ^{99m}Tc-Medronate (MDP) [Fig. 2(b)], and (2) a hot sphere phantom with uniform intensity of 11 embedded in the center of a uniform cylinder with intensity of 1, i.e., with the local contrast of 10:1 [Fig. 2(c)]. Using a 3D MPH analytical projector, we generated the MPH projections for different MPH pattern designs based on our former studies [3], [9], which were carefully investigated

to reduce axial distortions by providing more uniform axial sampling and avoid deterministic "ghost" artifacts resulting from inferior pinhole pattern designs in the reconstructed images, ranging from 1 to 13-pinholes (Fig. 3).

B. Multiplexing Schemes

As percentage of multiplexing is usually dependent on geometric parameters of the MPH design, e.g., pinhole pattern, pinhole numbers and magnification, we set up the imaging geometry differently by using different geometric parameters in three multiplexing schemes to generate various degrees of multiplexing. We generated noise-free and noisy projection images. The latter were obtained by simulating Poisson noise on differently scaled noise-free projections, yielding an ensemble of 20 noise realizations for each count level.

Multiplexing scheme (1): Fixed magnification and detection efficiency

We simulated a finite compact detector with a dimension of 12 cm × 12 cm and used a 22.5° rotated 4-pinhole pattern in the simulations [Fig. 3(b)]. We obtained 4 degrees of multiplexing (0%, 22.7%, 34% and 44.2%) in the projections by changing the scaling of the pinhole pattern as the positions of the pinhole apertures were simulated gradually closer to each other [Fig. 4(a) and (b)]. Both hot sphere and MOBY phantoms were used in this scheme and two projection count levels (1M and 4M) were simulated. The overlapping regions of the projection were identified on the projection images, and the degree of multiplexing is de-fined as shown in the equation at the bottom of the page.

Multiplexing scheme (2): Changed magnification with fixed detection efficiency

We obtained 4 degrees of multiplexing (0%, 24%, 41% and 61%) for the same detector size and pinhole pattern as in scheme (1) by changing the collimator length with fixed radius-of-rotation (ROR) and reconstructed pixel size of 0.3 mm under the same 4-pinhole pattern [Fig. 4(c) and (d)]. The patterns were also scaled slightly for each setting for optimally utilizing the whole detector area and its effect on detection efficiency has been assured to be ignorable. The MOBY phantom was used in this scheme with three projection count levels (0.25M, 1M, and 4M) simulated (Fig. 5).

Multiplexing scheme (3): Fixed magnification with changed detection efficiency

We obtained five degrees of multiplexing for a small compact camera and a conventional gamma camera by increasing the pinhole aperture number (Fig. 4(e) and (f)). For a small camera, we simulated 1, 4, 5, 7 and 9 pinholes and for a standard gamma camera, we simulated 1, 5, 7, 9 and 13 pinholes. The single pinhole case was used as a baseline reference for this study. The MOBY phantom was simulated in this scheme and all projections were generated under the same acquisition time and same ROR.

For single pinhole case, another shorter ROR (2.5 cm compared to 3.5 cm) was simulated for both compact camera and standard gamma camera, to provide a more realistic representation for single pinhole imaging when the projection utilizes the whole detector area.

$$\%\text{multiplexing} = \frac{\text{number of pixels with multiplexing in the projection}}{\text{number of pixels with non} - \text{zero value in the projection}}$$

A summary for the aforementioned simulation schemes is listed in Table I. We reconstructed the projection data with up to 100 iteration numbers using an iterative ML-EM

based 3D MPH reconstruction algorithm. To study the multiplexing effects independently, no other image degradation factors such as pinhole geometric blurring, attenuation or scatter were modeled in the projector and reconstruction method.

C. Data Analysis

We used the normalized-mean-square-error (NMSE), normalized-standard-deviation (NSD) and local contrast as the figures-of-merit to study and evaluate trade-offs among bias, noise and contrast in the reconstructed images for different multiplexing schemes. The whole reconstructed volume was used to assess the average NMSE.

$$\text{average NMSE}=\frac{1}{n}\sum_{j=1}^{n}\left(\frac{x_j-\lambda_j}{\bar{\lambda}}\right)^2 \tag{1}$$

n number of voxels in the whole reconstructed volume

λ voxel count value in the original phantom

$\bar{\lambda}$ mean voxel value of the original phantom

x voxel count value in the noise free reconstructed image

j voxel index

The NSD image was obtained based on the mean and variance reconstructed images obtained from the 20 noisy projection realizations. We then computed the mean value of the NSD in a 3D uniform region chosen close to the center of the object in the reconstructed image as the indicator of the noise level.

$$\text{average NSD}=\frac{1}{n}\sum_{j=1}^{n}\frac{\sqrt{\frac{1}{m-1}\sum_{i=1}^{m}(x_j^i-\overline{x_j})^2}}{\overline{x_j}} \tag{2}$$

m number of noise realizations

n number of voxels in the selected uniform region in the reconstructed image

x voxel count value in the noisy reconstructed image

$\bar{x}$ voxel count value in the mean reconstructed image

i noise realization index

j voxel index

The 3D local contrast was calculated from the chosen signal and background regions for different degrees of multiplexing and updates of the reconstructed images as shown in Fig. 6 in the hot sphere phantom simulation in scheme (1):

$$\text{Local contrast}=\frac{\text{Mean hot sphere}-\text{Mean background}}{\text{Mean background}} \tag{3}$$

III. RESULTS

Using our pre-determined pinhole-hole patterns, generally, no significant image distortions and artifacts were found on the reconstructed images for different degrees of multiplexing for all simulation schemes, demonstrating the effectiveness of the 3D MPH reconstruction method. Further discussion about the reconstruction problem for multiplexing MPH SPECT can be found in [9] and is beyond the scope of this paper. Increased degree of multiplexing showed increased bias in the reconstructed images in the early iteration number, and their discrepancy decreased for higher iterations for all schemes. Results from different noise levels were similar, all indicating that the gain of detection efficiency and resolution from MPH would be off-set by the increased image degradation from multiplexing. In the following we discussed some specific findings for each multiplexing scheme.

A. Multiplexing Scheme (1)—Multiplexing Effect Only

Since the magnification and detection efficiency were fixed in this scheme, how the multiplexing affected the reconstructed image quality was analyzed independently from other confounding factors. Our results showed that bias increased as the degree of multiplexing increased. However, the noise level slightly improved for higher degree of multiplexing as indicated by a decrease in the NSD values. The trade-off curves of bias and noise illustrated that less multiplexing provided better performance in terms of lowering noise and substantial artifacts (Fig. 7). Local contrast was analyzed in the hot sphere phantom simulation. The results showed that increased multiplexing did not significantly affect the image quality in terms of the trade-off between contrast and noise under this specific simulation setting (Fig. 8). Results of bias and noise trade-offs from both MOBY and hot sphere phantom for different count levels were similar (Fig. 9).

B. Multiplexing Scheme (2)—Multiplexing Combined With Magnification Effects

In this scheme, we studied how the multiplexing affected the image quality if its purpose is to improve image resolution. Different degrees of multiplexing were obtained from different magnification factors to investigate the effects of resolution and multiplexing simultaneously. Higher degree of multiplexing showed increased bias. However, after incorporating the improvement of resolution from a higher magnification, the differences of bias among different degree of multiplexing were more subtle as comparing to scheme (1). In this scheme, the bias of the reconstruction images with the smallest magnification factors and without any projection multiplexing was a bit higher than others at higher iterations, suggesting that resolution loss resulted from lower magnification was a more significant factor in bias as compared to the multiplexing effect in this case. The increased noise level for the settings of higher magnification and more multiplexing was due to more shared pixels by a given number of incident photons for a higher magnification setting. As a result, the statistical variations at each pixel increased, thus amplifying the reconstructed noise level given that the reconstructed voxel size was sufficiently small to realize the resolution difference in the projection domain [Fig. 10(b)]. The trade-off curves of bias and noise again showed that lower degree of multiplexing provided better performance in terms of bias and noise trade-off, and also indicated that the gain of resolution is offset by the increased image degradation or bias due to higher degree of multiplexing [Fig. 10(a)].The trade-offs of bias and noise for 0% and 24% multiplexing are comparable. Simulations with other noise levels of 1 M and 0.25M are similar (Fig. 11). This study found out that excessive multiplexing to pursue better resolution will lead to degradation in image quality in MPH collimator design.

C. Scheme (3)—Multiplexing Combined With Detection Efficiency Effects

In this scheme, we aimed to determine the optimal number of pinholes for both compact and conventional gamma cameras. Here, the motivation for multiplexing was to increase

detection efficiency. A greater number of pinholes improves photon counts but at the expense of a greater degree of multiplexing. Our results indicated that for both compact and conventional cameras, with careful consideration using a limited number of pinholes, MPH collimators offer significant advantages over single pinhole collimator in both reducing bias and improving noise for the same ROR. A single pinhole with a shorter ROR of 2.5 cm showed the least bias among all the pinhole configurations because of the highest resolution achieved. However, its overall bias-noise trade-off was still inferior to MPH designs. For standard gamma camera, the bias decreased for 5–9 pinholes comparing to single pinhole for the same ROR because of the improved axial sampling from the multi-pinhole, but the improvement is gradually offset by the increased bias from the increased multiplexing with increasing number of pinholes (13-pinhole). The noise level improved with a greater number of pinhole. A single pinhole with a smaller ROR resulted in the highest level of noise, which is again due to the higher magnification and the statistical variation for each pixel element increased. Our results indicated that improvement in detection efficiency by allowing some multiplexing is a reasonable strategy in MPH design but that an optimal number of pinholes exists beyond which further gain in detection efficiency is offset by a loss of image quality due to excessive multiplexing. We found out that the pinhole numbers that provided best trade-off in terms of noise and bias were 7 [Fig. 12(b)] for the compact 12 cm × 12 cm camera, and 9 [Fig. 12(a)] for the standard 40 cm × 40 cm gamma camera, base on this particular application.

IV. DISCUSSIONS

Multi-pinhole SPECT has become an evolving research area for small animal imaging in recent years, and unlike conventional SPECT scanners, there is no consensus on optimal MPH collimator design due to the vast number and intricate complexity of the design parameters. However, authors as well as other investigators studied about the relation between pinhole pattern and multiplexing [3], [6], [7]–[13] and found that for a combination of certain regular patterns, multiplexing can lead to an inferior MPH design in terms of “ghost” artifact generation. On the other hand, incomplete axial sampling can lead to axial distortion. In this study, we focused on quantifying the effect of multiplexing on the reconstruction image quality and investigated how it interplays with other parameters by setting up different simulation schemes, leading to the substantial clue for setting up the criteria for MPH design. This study excluded the effect of truncation artifacts, which is also highly related to multiplexing and will be studied in details in a separate paper from our laboratory. In scheme (1), we performed the simulations using two phantoms with different activity distributions and uptake ratios and showed consistent results. However, further study is needed to determine if the multiplexing effect is independent of the activity distribution.

We defined the degree of multiplexing in the projection domain as the area with overlapping over to the total projection area, without taking the order of multiplexing (how many pinhole apertures contribute to the area of overlapping) into consideration. This concept is more intuitive and practical for the collimator design. Vunckx *et al.* [6] suggested another definition of multiplexing in the reconstruction image domain. Although the definitions of multiplexing are different, the results from both studies are in general good agreement, indicating the utility of the concept.

The results from scheme (1) showed that multiplexing does not affect image contrast significantly. It can be attributed to the specific phantom used. Another observation is that an increase in image intensity in the signal area and a decrease in image intensity in the background area with higher degrees of multiplexing, resulting in an artifactual increase in

image contrast as compared to the truth. Additional simulations with different phantoms are needed to further investigate this phenomenon.

To validate the explanations of the results from scheme (2), we performed a set of single pinhole simulations using the hot sphere phantom with two different magnification factors by changing the collimator length. In Fig. 13, we showed the mean NSD over a uniform region in the reconstructed images increases asymptotically as a function of iteration number and the magnitude is generally higher for higher magnification. This can be explained by the spreading of the same total number of detected counts into more projection image pixels with increased magnification. Also, the results suggested that noise amplification is not a consequence of the increased degree of multiplexing in scheme (2).

There are several strategies to minimize or eliminate multiplexing: For the measured data, physical septa [4], [15] and the MPH collimator design itself, e.g., acceptance angle of the pinhole aperture, pinhole pattern, collimator length and pinhole number, etc., can be used. For simulations, some postprocessing techniques can be used after data acquisition [6]. The theoretical methods are assumed to be translatable to using the physical septa. We achieved this purpose in our study by changing the collimator design, which offers the advantage of easier implementation in the simulation. It is also more practical to obtain different field-of-views (FOVs) in the instrumentation design as a means for alleviating truncation artifacts for optimized reconstructed image quality. Overall, this study provides a general guideline for MPH collimator design prior to the use of computationally intensive task-based optimization methods, e.g., an ROC study [16], to determine the optimized MPH collimator design.

V. CONCLUSIONS

We have quantified the effects of multiplexing in terms of trade-off among bias, noise and contrast in the reconstructed images. Our results suggest that the gains in detection efficiency and resolution from increased multiplexing are offset by increased image degradation in terms of bias and noise. We have also determined the optimal pinhole number is about 7 for a compact camera with size of 12 cm × 12 cm and 9 for a standard gamma camera with size of 40 cm × 40 cm using the MOBY phantom with bone scan distribution. Excessive multiplexing to improve image resolution would not improve the overall trade-off of bias and noise compared to those without any projection multiplexing. However, when comparing to no degree of multiplexing, the trade-off improves initially with increased multiplexing by allowing more number of pinholes to improve detection efficiency. The trade-off then reached a maximum and decreased with further multiplexing due to image degradation from increased bias and artifacts in the reconstructed MPH images. Although the aforementioned factors are complex, they must be considered in the optimum MPH collimator design for small animal SPECT imaging.

Acknowledgments

This work was supported by the NIH research grant EB001558.

References

1. Jaszczak RJ, Li JY, Wang HL, Zalutsky MR, Coleman RE. Pinhole collimation for ultra-high-resolution, small-field-of-view Spect. Phys Med Biol. 1994; 39:425–437. [PubMed: 15551591]
2. Meikle SR, Kench P, Kassiou M, Banati RB. Small animal SPECT and its place in the matrix of molecular imaging technologies. Phys Med Biol. 2005; 50:R45–R61. [PubMed: 16264248]
3. Mok, GSP.; Tsui, BMW.; Wang, Y.; Du, Y.; Segars, W.; Frey, E. Effects of pinhole pattern and multiplexing in multi-pinhole small animal SPECT. presented at the 52nd Ann. Meet. Soc. Nucl. Med; Toronto, Canada. 2005.

4. Beekman FJ, Vastenhouw B. Design and simulation of a high-resolution stationary SPECT system for small animals. Phys Med Biol. 2004; 49:4579–4592. [PubMed: 15552418]
5. Schramm NU, Ebel G, Engeland U, Schurrat T, Behe M, Behr TM. High-resolution SPECT using multi-pinhole collimation. IEEE Trans Nucl Sci. Jun; 2003 50(3):315–320.
6. Vunckx K, Suetens P, Nuyts J. Effect of overlapping projections on reconstruction image quality in multi-pinhole SPECT. IEEE Trans Med Imag. Jul; 2008 27(7):972–983.
7. Segars WP, Tsui BMW, Frey EC, Johnson GA, Berr SS. Development of a 4-D digital mouse phantom for molecular imaging research. Molecular Imag Biol. 2004; 6:149–159.
8. Cao Z, Bal G, Accorsi R, Acton PD. Optimal number of pinholes in multi-pinhole SPECT for mouse brain imaging-a simulation study. Phys Med Biol. 2005; 50(19):4609–4624. [PubMed: 16177493]
9. Wang, Y.; Tsui, BMW. Application of crosstalk concept to assessment of multi-pinhole collimator designs in small animal SPECT imaging. presented at the IEEE Nucl. Sci. Symp. Med. Imag. Conf; San Diego, USA. 2006.
10. Vunckx K, Beque D, Defrise M, Nuyts J. Single and multipinhole collimator design evaluation method for small animal SPECT. IEEE Trans Med Imag. Jan; 2008 27(1):36–46.
11. Wilson DW, Barrett HH, Clarkson EW. Reconstruction of two- and three-dimensional images from synthetic-collimator data. IEEE Trans Med Imag. May; 2000 19(5):412–422.
12. Bal G, Zeng GL, Lewitt RM, Cao Z, Acton PD. Study of different pinhole configurations for small animal tumor imaging. Proc IEEE Nucl Sci Symp Conf Rec. 2004; 5:3133–3137.
13. Vunckx K, Nuyts J, Vanbilloen B, Saint-Hubert MD, Vanderghinste D, Rattat D, Mottaghy FM, Defrise M. Optimized multipin-hole design for mouse imaging. Proc IEEE Nucl Sci Symp Conf Rec. 2008:4742–4750.
14. Meikle SR, Kench P, Weisengberger AG, Wojcik R, Smith MF, Majewski S, Eberl S, Fulton RR, Rosenfeld AB, Fulham MJ. A prototype coded aperture detector for small animal SPECT. IEEE Trans Nucl Sci. Oct; 2002 49(5):2167–2171.
15. Beekman FJ, van der Have F, Vastenhouw B, van der Linden AJA, van Rijk PP, Burbach JPH, Smidt MP. U-SPECT-I: A novel system for submillimeter-resolution tomography with radiolabeled molecules in mice. J Nucl Med. 2005; 46:1194–1200. [PubMed: 16000289]
16. Metz CE. ROC methodology in radiologic imaging. Invest Radiol. Sep; 1986 21(9):720–733. [PubMed: 3095258]

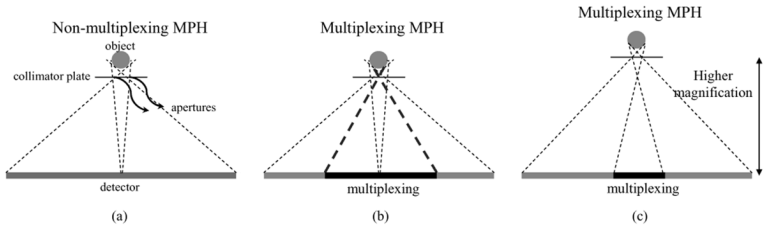

Fig. 1.

When comparing to non-multiplexing MPH design (a), which was a simplified 2-pinhole configuration here, multiplexing can improve (b) detection efficiency as more pinholes (3 pinholes here) can be packed or can improve (c) resolution in the projection domain since each projection shares more detector pixel elements by allowing a higher magnification.

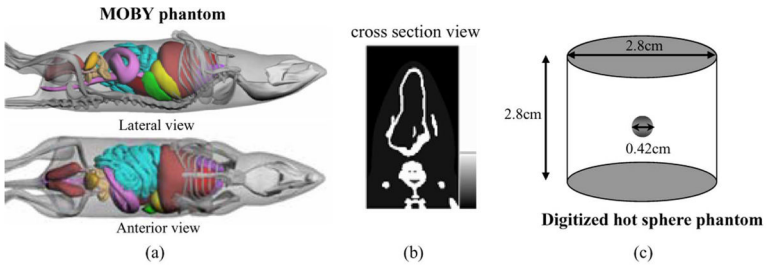

Fig. 2.

Two digitized phantoms were used in this simulation study. (a) The digital mouse whole body (MOBY) phantom that realistically models the anatomy of a normal C57BL/6 mouse, with a typical bone study activity distribution of ^{99m}Tc-MDP (b), and (c) a hot sphere phantom embedded in the center of a uniform cylinder with a local contrast of 10:1.

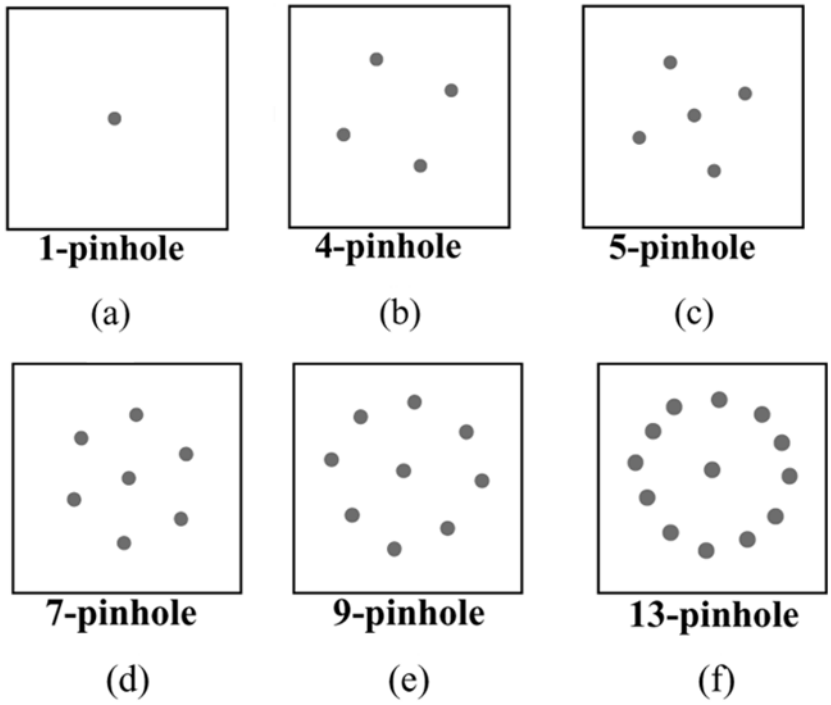

Fig. 3.
Some sample pinhole patterns that were used in the study, ranging from 1 (a) to 13 (f) pinholes.

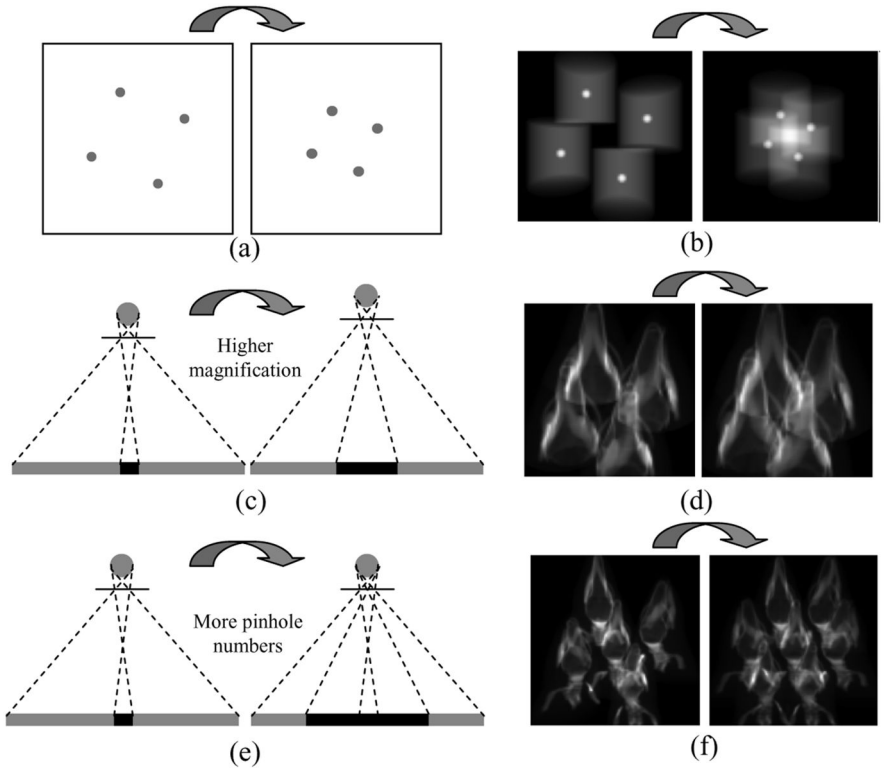

Fig. 4.

We obtained different degrees of multiplexing from three multiplexing schemes: (a) Scheme (1)—fixed magnification and detection efficiency with different scaling of the same pinhole pattern and their corresponding sampled projection images (b). (c) Scheme (2)—fixed detection efficiency and changed magnification by changing the collimator length and their corresponding sampled projection images (d). (e) Scheme (3)—fixed magnification and changed detection efficiency by adding more pinholes and its corresponding sampled projection images (f).

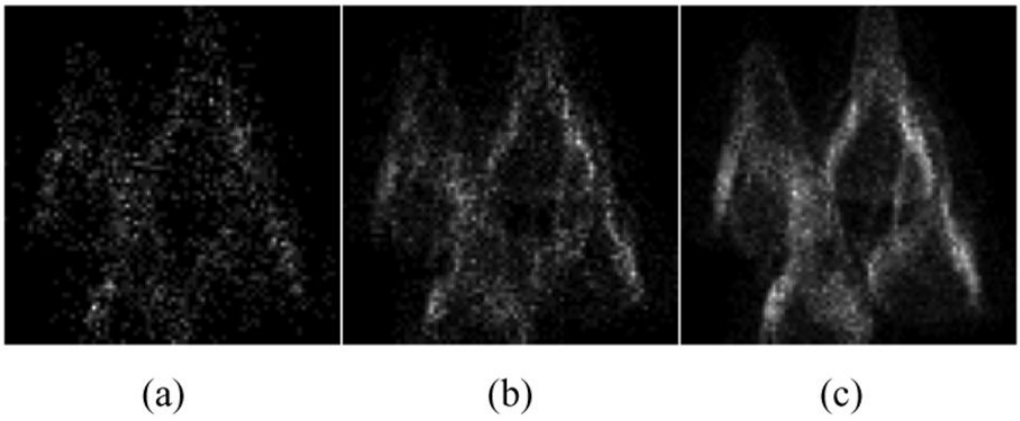

Fig. 5.
We simulated 3 different noise levels by adding the Poisson noise on the noise free projections with 3 different total count levels: (a) 0.25M, (b) 1M and (c) 4M in scheme (2).

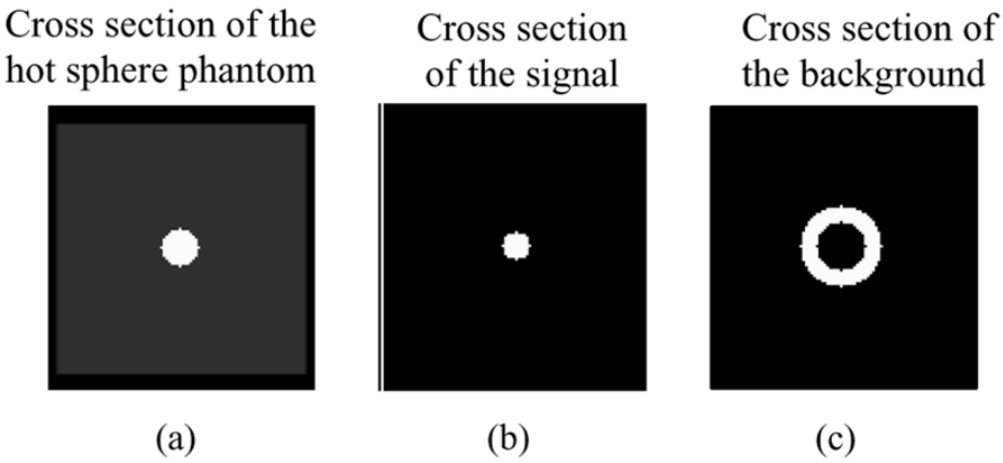

Fig. 6.

The 3D local contrast was calculated for different degrees of multiplexing in the hot sphere simulation study in Scheme (1). (a) The cross section of the original phantom. (b) The cross section of the chosen signal region, whose radius was 3 pixels shorter than the original phantom to eliminate the numerical errors on the edge of the reconstructed images. (c) The cross section of the chosen hollow sphere as the background region for calculating the contrast. The inner radius was also 3 pixels larger than the hot sphere phantom to avoid numerical errors.

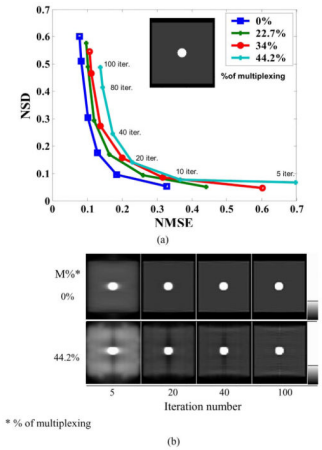

Fig. 7.

The trade-off of bias and noise was plotted for different degrees of multiplexing, i.e., 0%, 22.7%, 34% and 44.2% in scheme (1) for the hot sphere phantom simulation (a). Results indicated that bias increased and noise level slightly improved for a higher degree multiplexing for different iteration number. A lower degree of multiplexing offered a better performance for scheme (1). (b) Sampled noise free reconstruction images of different iterations matched with the findings in (a) as the artifacts are more prominent in the early iterations for a higher degree of multiplexing. The projection count level for the noise study (NSD) is 4M.

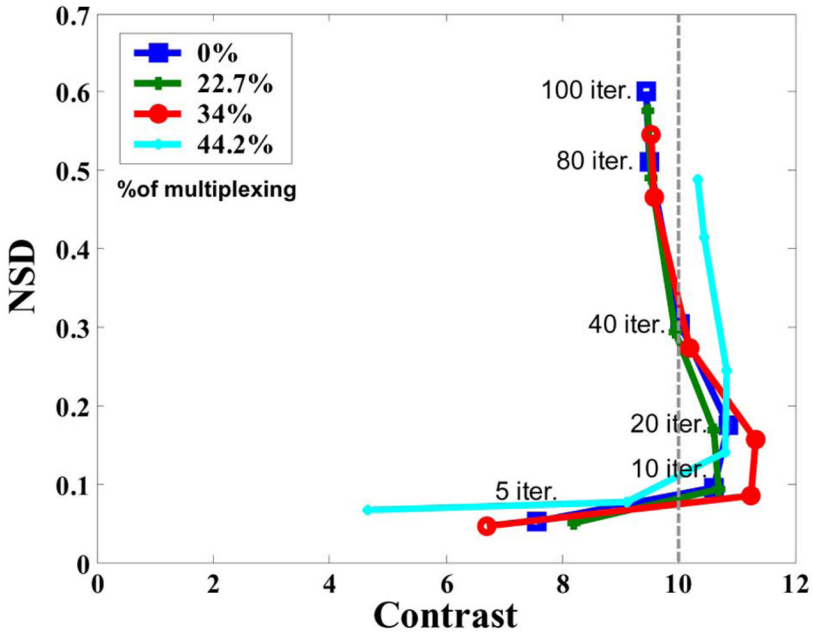

Fig. 8.

In terms of contrast-to-noise trade-offs, results from different degrees of multiplexing are not significantly different in simulation scheme (1). Highest degree of multiplexing (44.2%) needs more number of iteration to approach the real contrast (10:1) as shown in the vertical dash line.

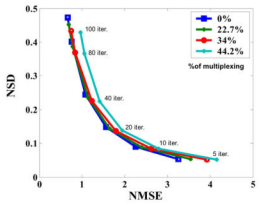

Fig. 9.

Results of the MOBY phantom simulation from scheme (1) matched with those of the hot sphere phantom simulation. The trade-off of bias and noise showed that a lower degree of multiplexing offers a better performance. The projection count level for the noise study is 1M and the legends mean the % of multiplexing.

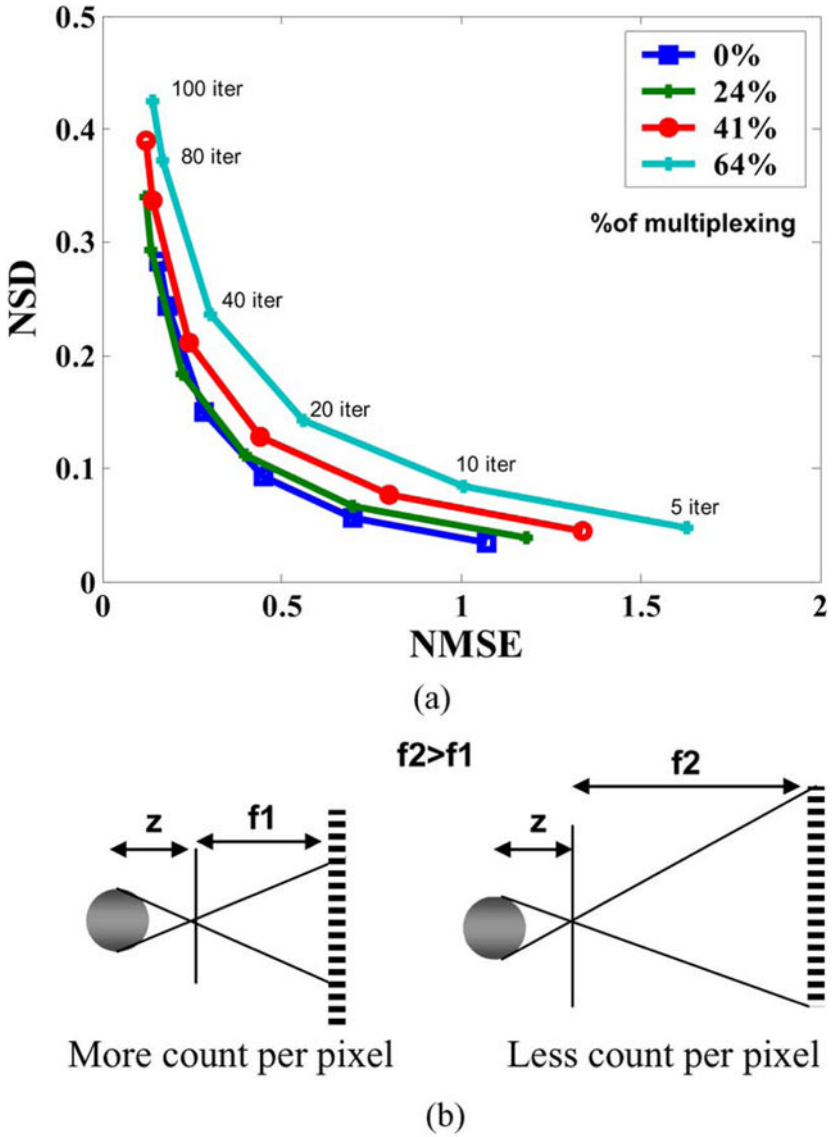

Fig. 10.

(a) The bias and noise trade-offs were plotted for different degrees of multiplexing, i.e., 0%, 24%, 41% and 61% in scheme (2) with the MOBY phantom simulation. The bias increased for higher degree of multiplexing but their differences were smaller comparing to scheme (1). The noise level increased for a higher degree multiplexing here which is opposite to scheme (1), since more pixel elements shared a given number of incident photons at a higher magnification setting and the statistical variation for each pixel element increased as explained in (b). The projection count level for the noise study is 4M. The trade-off of bias and noise again showed that a lower degree of multiplexing offered a better performance.

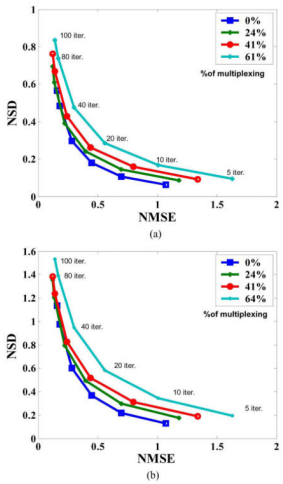

Fig. 11.

Simulations with other noise levels: (a) 1 M & (b) 0.25M in scheme (2) also showed similar results that a lower degree of multiplexing offered a better performance in terms of bias and noise trade-offs.

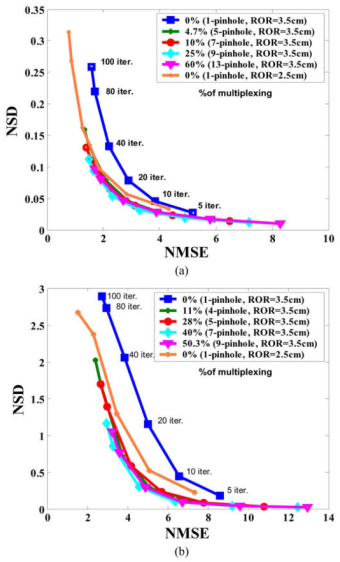

Fig. 12.

The bias and noise trade-offs were plotted for different degrees of multiplexing for scheme (3) with MOBY phantom simulation. (a) *Standard gamma camera*: The trade-off of bias and noise showed that the optimal number of pinhole for a standard gamma camera was about 9. (b) *Compact gamma camera*: The trade-off of bias and noise curves showed that the optimal number of pinholes for a compact gamma camera was about 7). All projections were generated with the same acquisition time.

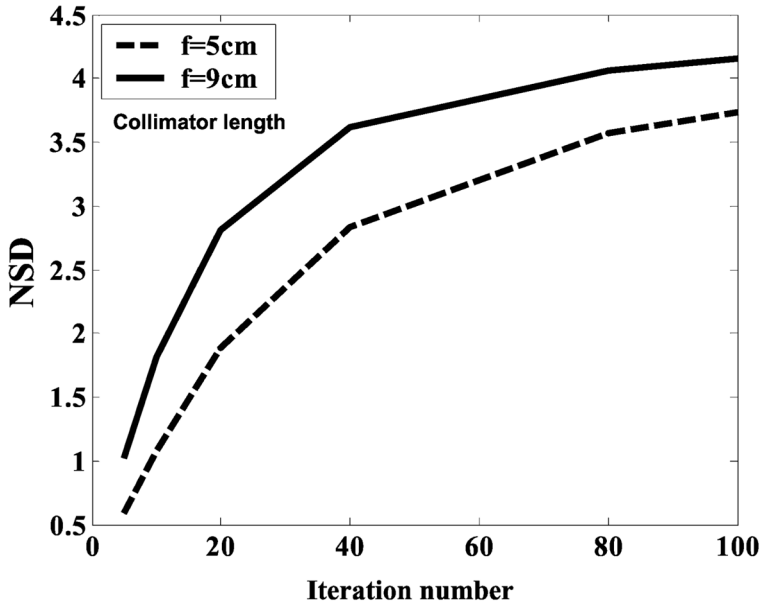

Fig. 13.

The single pinhole simulations using the hot sphere phantom for justifying our explanation in scheme (2). The different collimator lengths were simulated (5 cm and 9 cm) and the results showed that the noise increased asymptotically as a function of iteration number and the magnitude is generally higher for a higher magnification. This can be explained as given number of counts spread out in more pixel elements in the projections for higher magnification.

TABLE I

Summary of the Simulation Setup for Three Multiplexing Schemes

	Phantom	No. of pinholes	ROR (cm)	Collimator (cm)	% of multiplexing	Count level	Detector size	Note
Scheme (1)	MOBY / Hot sphere	4	4.8	7	0, 22.7, 34, 44.2	1M, 4M	12cm×l2cm	Same magnification and detection efficiency
Scheme (2)	MOBY	4	3	5,7,8,10	0,24,41,61	0.25M, 1M, 4M	12cm×l2cm	Same detection efficiency with changed magnification
Scheme (3)	MOBY	1,5,7,9,13 / 1,4,5,7,9	2.5*/3.5	14 / 7	0,4,7,10,25,60 / 0,11,28,40,50,3	Same acq. time	40cm×40cm / 12cm×12cm	Same magnification with changed detection efficiency

*2.5cm for single pinhole imaging geometry only